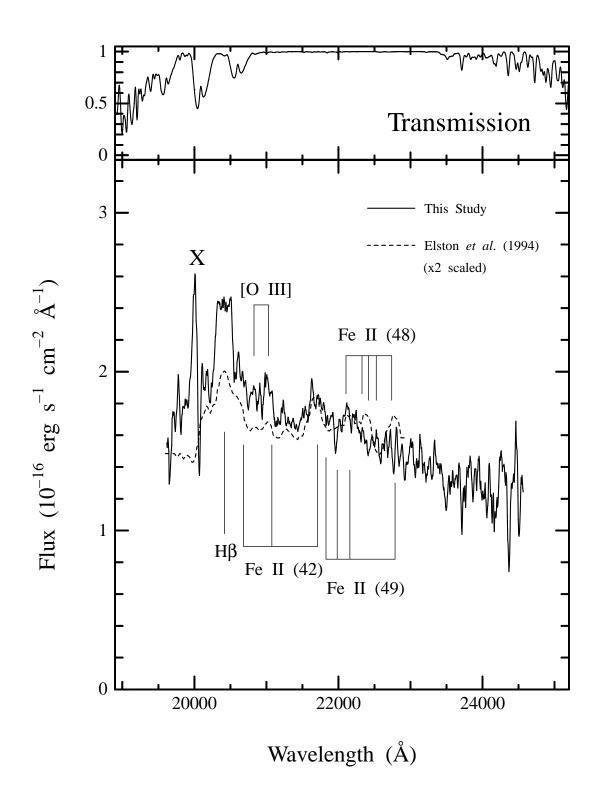
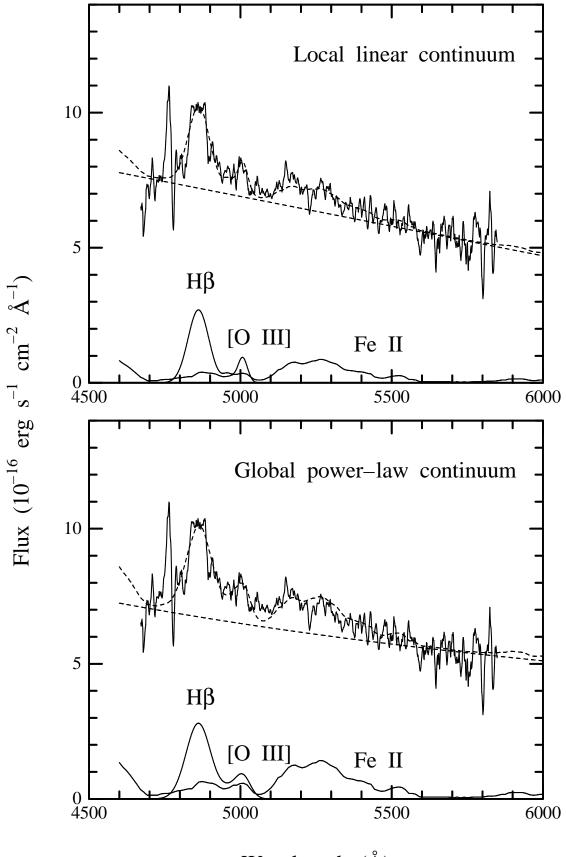
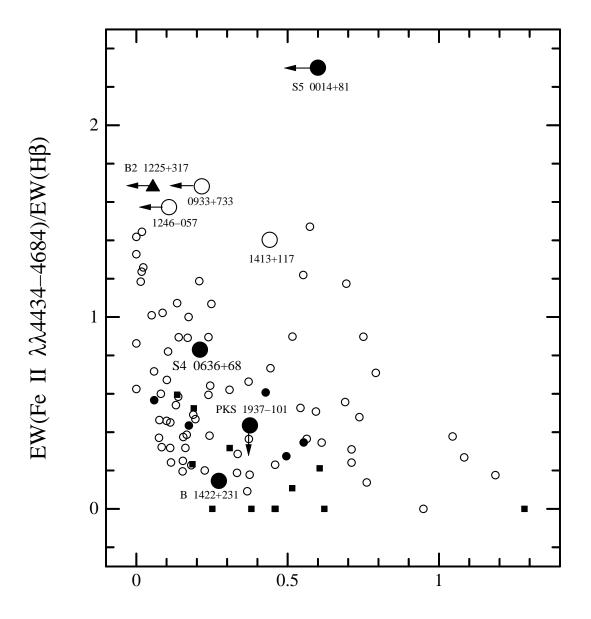


Wavelength (Å)

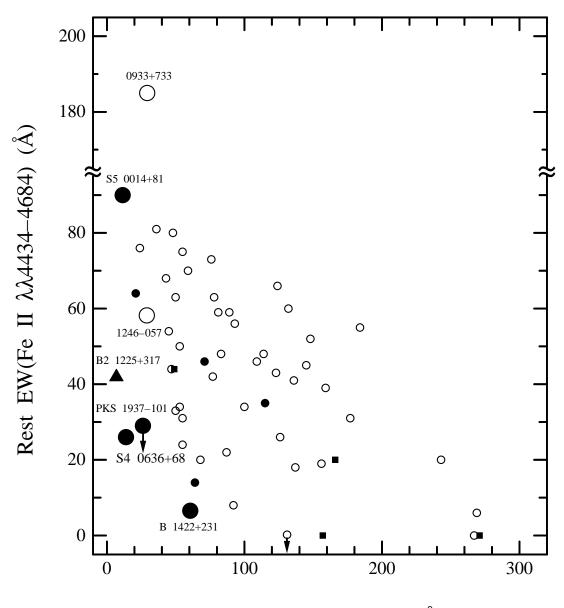




Wavelength (Å)



EW([O III] $\lambda 4959 + \lambda 5007)/EW(H\beta)$



Rest EW(CIV $\lambda 1549$) (Å)

NEAR-INFRARED SPECTROSCOPY OF THE HIGH REDSHIFT QUASAR S40636+68 AT z=3.2

TAKASHI MURAYAMA¹ AND YOSHIAKI TANIGUCHI¹ Astronomical Institute, Tohoku University, Aoba, Sendai 980-8578, Japan Electronic mail: murayama@astr.tohoku.ac.jp, tani@astr.tohoku.ac.jp

AARON S. EVANS¹

California Institute of Technology, 105-24, Pasadena, CA 91125 Electronic mail: ase@astro.caltech.edu

D. B. SANDERS

Institute for Astronomy, University of Hawaii, 2680 Woodlawn Drive, Honolulu, HI 96822 Electronic mail: sanders@ifa.hawaii.edu

Youichi Ohyama¹

Astronomical Institute, Tohoku University, Aoba, Sendai 980-8578, Japan Electronic mail: ohyama@astr.tohoku.ac.jp

Kimiaki Kawara and Nobuo Arimoto

Institute of Astronomy, The University of Tokyo, 2-21-1 Osawa, Mitaka, Tokyo 181-8588, Japan Electronic mail: kkawara@mtk.ioa.s.u-tokyo.ac.jp, arimoto@mtk.ioa.s.u-tokyo.ac.jp

To appear in the Astronomical Journal

ABSTRACT

We present near-infrared (observed frame) spectra of the high-redshift quasar S40636+68 at z = 3.2 which was previously thought to be one of a group of "strong" Fe II emitters (i.e., $F(\text{Fe II }\lambda\lambda4434-4684)/F(\text{H}\beta) > 1$). Our K-band spectrum clearly shows emission lines of H β and [O III] $\lambda\lambda4959$, 5007 as well as optical Fe II emission. Our computed value of $F(\text{Fe II }\lambda\lambda4434-4684)/F(\text{H}\beta) \simeq 0.8$ for S40636+68 is less than previously thought, and in fact is comparable to values found for radio-loud, flat-spectrum, low-z quasars. Therefore S40636+68 appears not to be a strong optical Fe II emitter. Although more than half (5/8) of the high-z quasars observed to date are still classified as strong optical Fe II emitters, their Fe II/H β ratios, for the most part, follow the same trend as that of low-z quasars, i.e., an anticorrelation in $EW(\text{Fe II})/EW(\text{H}\beta)$ versus $EW([\text{O IIII}])/EW(\text{H}\beta)$, with radio-loud quasars having a mean value of $EW(\text{Fe II})/EW(\text{H}\beta)$ approximately half that of radio-quiet quasars at comparable values of $EW([\text{O IIII}])/EW(\text{H}\beta)$.

¹Visiting Astronomer of the University of Hawaii 2.2 meter telescope.

1. INTRODUCTION

Since optical Fe II emission² is often one of the prominent features in the spectra of Type 1 active galactic nuclei (AGN), it is perhaps not surprising that several observational and theoretical studies have been made to explain the strength of this feature in quasars (e.g. Phillips 1977, 1978; Kwan & Krolik 1981; Netzer & Wills 1983; Wills *et al.* 1985; Collin-Souffrin *et al.* 1988; Zheng & O'Brien 1990; Joly 1991; Boroson & Green 1992; Lípari *et al.* 1993; Wang *et al.* 1996a). Although it is known that the strength of the optical Fe II emission shows an anticorrelation with the strength of [O III] emission (Boroson & Green 1992), the physical properties of the Fe II emitting region are not yet fully understood.

Recent near-infrared (NIR) spectroscopic studies by Hill *et al.* (1993) and Elston *et al.* (1994; hereafter ETH) suggest that unusually strong optical Fe II emitters may be common in the high-*z* universe (2 < z < 3.4). Though it is known that some low-*z* far-infrared (FIR) selected AGN ($L_{\text{FIR}} \geq 10^{11} L_{\odot}$) show strong Fe II emission in their optical spectra (cf. Lípari *et al.* 1993), such extreme Fe II emitters appear to be rare in the low-*z* universe. Recently, we obtained NIR spectra of two radio-loud, flat-spectrum, high-*z* quasars (B 1422+231 at *z* = 3.6 and PKS 1937–101 at *z* = 3.8) and found that their flux ratios of *F*(Fe II $\lambda\lambda4434-4684$)/*F*(H β) are much less than those of the other high-*z* quasars (Kawara *et al.* 1996; Taniguchi *et al.* 1996, 1997), and in fact are similar to those of radio-loud, flat-spectrum, low-*z* quasars with normal optical Fe II emission. These new observations suggest that high-*z* quasars may exhibit a range of values of *F*(Fe II $\lambda\lambda4434-4684$)/*F*(H β) similar to what has been observed for low-*z* quasars.

If the strong Fe II emission could be attributed to the overabundance of iron, host galaxies of the high-z quasars with strong Fe II emission would form at $z \sim 10$ because it is usually considered to be the case that the bulk of the iron arises from Type Ia supernovae which occur $\sim 1-2$ Gyr after the first major epoch of star formation (e.g., Hamann & Ferland 1993, Yoshii *et al.* 1996). It is therefore important to investigate the chemical properties of high-z quasars systematically.

In this paper we present new NIR spectroscopy of S40636+68, a flat-spectrum radio-loud quasar at z = 3.2, which is reported in ETH as a very strong iron emitter. Based on our new measurements, we discuss whether the fraction of high-z quasars with strong optical Fe II emission is substantially higher than that of low-z quasars.

²The Fe II emission feature actually extends from the near-UV into the red optical region of the spectrum. However, following previous convention, we use the term "optical Fe II emission" in this paper to mean the Fe II emission near H β (i.e., Fe II $\lambda\lambda$ 4434–4684).

2. OBSERVATIONS AND DATA REDUCTION

We observed S40636+68 on 1996 April 7 (UT) using the K-band spectrograph (KSPEC; Hodapp *et al.* 1994) at the Cassegrain focus (f/31) of the University of Hawaii (UH) 2.2 m telescope in combination with the UH tip-tilt system (Jim *et al.* 1997). The cross-dispersed echelle design of KSPEC provided simultaneous coverage of the entire 1–2.5 μ m wavelength region. The projected pixel size of the HAWAII 1024 × 1024 array was 0.167 along the slit and $\simeq 5.6$ Å at 2 μ m along the dispersion direction. We used a 0.96 wide slit oriented East-West and centered on the intensity peak of the object. Twenty exposures, each of 180 sec integration under photometric conditions, were obtained by shifting the position of the object along the slit at intervals of 5" between each integration. The total integration time was 3600 sec. An A-type standard star, HD 106965 (Elias *et al.* 1982), was observed for flux calibration. Another A-type standard star, HD 1166965 (Elias *et al.* 1982), was also observed before and after observing S40636+68 in order to correct for atmospheric absorption. Spectra of an incandescent lamp and an argon lamp were taken for flat-fielding and wavelength calibration, respectively. Typical widths of the spatial profiles of the standard star spectra were ~ 0.5 (FWHM) throughout the night.

Data reduction was performed with IRAF³ using standard procedures as outlined in Hora & Hodapp (1996). Sky and dark counts were removed by subtracting the average of the preceding and following exposures, and then the resulting frame was divided by the normalized dome flat. The target quasar was not bright enough to trace its position in each frame with sufficient accuracy. Therefore, at first, we fit the spectral positions of the standard star spectra with a third-order polynomial function which properly traces the echelle spectrum. These fitting results were then applied to the quasar spectra. Using this procedure, we extracted the quasar spectra with an aperture of 3" which was determined to be the typical width where the flux was $\sim 10\%$ of the peak flux along the spatial profile of the standard star. In order to subtract the residual sky emission, we used the data just adjacent to the 3'' aperture. The wavelength scale of each extracted spectrum was calibrated to an accuracy of 18 km s⁻¹ at 1.1 μ m, 20 km s⁻¹ at 1.6 μ m, and 19 km s⁻¹ at 2.0 μ m, respectively, based on both the argon emission lines of the calibration lamp and on the telluric OH emission lines. The spectral resolutions (FWHM) measured from the argon lamp spectra were $\simeq 500$ km s⁻¹ at 1.1 μ m, $\simeq 450$ km s⁻¹ at 1.6 μ m, and $\simeq 500$ km s^{-1} at 2.0 μ m. The spectra were finally median combined in each band. Atmospheric absorption features were removed using the spectra of the A-type star HD 136754 because A-type stars are best suited for correcting for atmospheric absorption features. However, since A-type stars inherently have hydrogen recombination absorption lines (e.g., the Brackett series in H and Kbands and the Paschen series in I and J bands), we removed these features before the correction using Voigt profile fitting. In order to check whether this procedure worked we also applied the

³Image Reduction and Analysis Facility (IRAF) is distributed by the National Optical Astronomy Observatories, which are operated by the Association of Universities for Research in Astronomy, Inc., under cooperative agreement with the National Science Foundation.

same atmospheric correction for the spectra of M-type stars whose data were obtained on the same night. Comparing our corrected spectra of the M-type stars with their published spectra (Lançon & Rocca-Volmerange 1992), we found that our correction procedure works appropriately. Finally, in order to calibrate the flux scale, we used the spectrum of the standard star HD 106965 (A2, K=7.315) divided by a 9000 K blackbody spectrum, which fits the *JHKL* magnitude of the standard (Elias *et al.* 1982) with only 1.2% deviation. Photometric errors were determined to be < 10% over all observed wavelengths.

3. RESULTS AND DISCUSSION

3.1. The Rest-Frame UV and Optical Spectra of S40636+68

Figure 1 shows the spectra of S40636+68 (solid line) in the *IHK* bands together with the Large Bright Quasar Survey (LBQS) composite spectrum (dashed line; Francis *et al.* 1991) shifted to z = 3.2. The atmospheric transmission of Mauna Kea is shown in the upper panel. The spectrum clearly shows H β at 2.04 μ m and a broad "bump" of Fe II emission between 2.15 μ m and 2.23 μ m. The spike feature in our spectrum marked by 'X' is caused by residual atmospheric absorption. Although ETH did not find evidence for [O III] $\lambda\lambda$ 4959, 5007 emission lines, our *K*-band spectrum shows their presence (which will be discussed later). No prominent emission lines were found in the *I*-, *J*-, and *H*-band regions of the spectrum. Mg II λ 2798 would be expected to appear at ~ 1.18 μ m but the *J*-band spectrum (not shown in Figure 1) was too noisy to be able to study Mg II. Since the efficiency of KSPEC in the *J*-band is not high, we do not use the *J*-band data in this paper.

In Figure 2, we compare our results with previous optical-NIR spectroscopic studies of S40636+68 (Sargent et al. 1989; Bechtold et al. 1994; ETH). Their basic data are summarized in Table 1. Our K-band spectrum is twice as bright as that of ETH. On the other hand, our I-band spectrum is 40% fainter than that of Bechtold *et al.* (1994). These flux discrepancies may be due to possible time variation inherent in the object or to calibration errors in the absolute photometry. However, since the two optical spectra taken at different observing dates over two years are quite consistent with each other (Sargent et al. 1989; Bechtold et al. 1994), it seems unlikely that this quasar is highly variable. Therefore, we consider the possibility that the discrepancy may be mostly due to calibration errors. First, we note that our *IHK* spectra were taken simultaneously and thus there is no internal calibration error in our spectra. Second, the optical spectra of Sargent et al. (1989) and Bechtold et al. (1994) show good agreement with each other and thus their photometric calibration seems reliable. Further, the optical power-law slope, $\alpha = -0.68 \ (f_{\nu} \propto \nu^{\alpha})$, given in Sargent *et al.* (1989) can be consistently extrapolated onto our K-band spectrum; the spectral index using the emission-free regions in both the optical spectrum (Sargent et al. 1989) and our K-band spectrum (1330–1380 Å, 1430–1460 Å, and 5400–5850 Å in the rest frame) is estimated to be $\alpha = -0.69$. Since the seeing during our observations was $\simeq 0.5^{\circ}$

(FWHM) and our slit size was 1", we think that we have detected nearly all of the light from the quasar. Though the details of the observing conditions and slit size are not given in ETH (see Table 1), seeing conditions on Mauna Kea are often better than at KPNO, judging from our experience at KPNO (see Kawara *et al.* 1996; Taniguchi *et al.* 1997), and, therefore we expect that our new measurement is more reliable.

3.2. The Rest-frame Optical Emission-line Properties of S40636+68

The main aim of our current observations is to provide a more accurate measure of the optical Fe II/H β ratio in S40636+68. Figure 3 compares our result with that of the ETH. (Note that the flux of ETH spectrum is scaled by a factor of two for proper comparison.) Center positions of H β , [O III] $\lambda\lambda$ 4959, 5007, and the Fe II multiplet (42) at a redshift z = 3.2 are marked in Figure 3. The peak positions of H β , [O III] $\lambda\lambda$ 4959, 5007, and Fe II $\lambda\lambda$ 4959, 5007, and Fe II multiplet 42 lines), coincide between the two spectra. The K-band spectrum of ETH appears to be dominated by very strong Fe II emission with weak, or nondetected [O III] $\lambda\lambda$ 4959, 5007. ETH actually stated that [O III] $\lambda\lambda$ 4959, 5007 was not detected, although they noted that their spectrum had small bumps of low significance at the position of the [O III] lines. On the other hand, our K-band spectrum clearly shows emission peaks which can be identified with [O III] $\lambda\lambda$ 4959, 5007.

To measure the Fe II fluxes in our spectrum, we fit emission-line features simultaneously with a least-squares algorithm. Such fitting results depend on the adopted continuum spectrum. As shown in Boroson & Green (1992), a local linear continuum is usually adopted to fit H β , [O III] $\lambda\lambda$ 4959, 5007, and the Fe II features. However, we have already obtained a global power-law continuum using the rest-frame UV and optical spectra as shown in Figure 2. Therefore, we performed spectral fitting for two cases; 1) local linear continuum and 2) global power-law continuum. In the fitting procedure, we assumed $F([O III] \lambda5007)/F([O III] \lambda4959)$ = 2.97 (Osterbrock 1989). We also assumed that the emission line profiles of H β and the [O III] $\lambda\lambda$ 4959, 5007 doublet are Gaussian. As for the optical Fe II emission features, we used an Fe II spectrum of a low-z BAL quasar, PG 0043+039 (Turnshek *et al.* 1994), as our Fe II template. All the emission lines are assumed to have the same redshift. Since it is known that high-ionization broad lines (e.g., C IV λ 1549) are often blueshifted with respect to low-ionization lines (Gaskell 1982; Wilkes 1984; Carswell *et al.* 1991; Nishihara *et al.* 1997 and references therein), we use only low ionization lines in our analysis.

The fitting results are presented in Figure 4 and Table 2 for each of the two assumed continua. The difference in the line flux ratios between the two cases is less than the measurement errors. Although we do not know which continuum case is more realistic, we adopt the results using the linear continuum fit for further discussion in order to compare our results with those of Boroson & Green (1992) and Hill *et al.* (1993) since they also adopted a local linear continuum.

In order to examine whether or not the detection of the [O III] lines are real in our spectrum, we compare our fit including the [O III] doublet with a fit excluding the [O III] doublet, where the local linear continuum has been adopted in both fits. A F-statistics test indicates that the fit with [O III] is improved over the 4900–5050 Å region from the fit excluding [O III] at a significance level of 99.8 %. Therefore, we conclude that the "bumps" at the [O III] positions are really the [O III] $\lambda\lambda$ 4959, 5007 doublet rather than Fe II $\lambda\lambda$ 4924, 5018 of the 42 multiplet. We obtained an average redshift $z = 3.200 \pm 0.002$.

Our fit assuming a local linear continuum gives the flux ratio $F(\text{Fe II } \lambda 5169)/F(\text{H}\beta) = 0.28$. This value is significantly smaller than the value of 0.45 that we estimate from the published spectrum of ETH. Although we do not understand this difference, it could reasonably be explained by uncertainties in the continuum fits between the two observations. However, we cannot rule out the possibility of time variation. In fact, such a time variation of Fe II is reported for the nearby type 1 Seyfert galaxy NGC 5548 (Wamsteker *et al.* 1990; Maoz *et al.* 1993; Sergeev *et al.* 1997). Thus, monitoring of S40636+68 may be needed in the future.

The flux ratio, $F(\text{Fe II }\lambda\lambda3500-6000)/F(\text{H}\beta)$, for S40636+68 is 3.5 ± 1.1 (Table 2). This value is greater than the mean value of 1.63 ± 0.88 for the six low-z quasars studied by Wills *et al.* (1985) and the value of 2.9 for 3C 273 which is the strongest optical Fe II quasar in the sample of Wills *et al.* (1985). However, $F(\text{Fe II }\lambda\lambda4434-4684)/F(\text{H}\beta)$ for S40636+68 is 0.83 ± 0.26 which is only half of the average value of 1.77 ± 0.17 for the four high-z quasars studied by Hill *et al.* (1993). Lípari *et al.* (1993) defined quasars with $F(\text{Fe II }\lambda\lambda4434-4684)/F(\text{H}\beta) \gtrsim 1$ as "strong" iron emitters. According to this criterion, we conclude that S40680+68 is not a strong Fe II emitter, contrary to the conclusion of ETH.

3.3. Statistical Properties of High-z Quasars vs. Low-z Quasars

In order to assess the significance of our new result for the ratio $F(\text{Fe II }\lambda\lambda4434-4684)/F(\text{H}\beta)$ in S40680+68 we first compare the rest-frame optical emission line properties of low-z and high-z quasars. Figure 5 shows the relationship of equivalent width (EW) ratios between $EW([\text{O III}] \lambda4959 + \lambda5007)/EW(\text{H}\beta)$ and $EW(\text{Fe II }\lambda\lambda4434-4684)/EW(\text{H}\beta)$ for low-z and high-z quasars compiled from the literature (Boroson & Green 1992; Hill *et al.* 1993; ETH; Kawara *et al.* 1996; Taniguchi *et al.* 1997). There is a distinct anticorrelation for the low-z quasars as noted before (cf. Boroson & Green 1992) although the reason for the anticorrelation between [O III] $\lambda\lambda4959$, 5007 and optical Fe II $\lambda\lambda4434-4684$ is still unknown. The low-z radio-loud quasars tend to have small ratios both in $EW([O III] \lambda4959 + \lambda5007)/EW(\text{H}\beta)$ and $EW(\text{Fe II }\lambda\lambda4434-4684)/EW(\text{H}\beta)$. Five of the eight high-z quasars show strong Fe II (i.e., Fe II/H $\beta > 1$) emission. The remaining three high-z quasars, which have Fe II/H $\beta < 1$, are all radio-loud and lie within the locus of values traced by low-z radio-loud quasars in Figure 5⁴. Also, the three radio-quiet quasars among the five high-z quasars with strong Fe II emission appear to lie within the upper envelope of values observed for low-z radio-quiet quasars. In summary, although over half (5/8) of the high-z quasars appear to be by definition strong Fe II emitters, all but two (the radio-loud Fe II quasars S50014+81 and B21225+317: ETH; Hill *et al.* 1993) of the high-z quasars follow a similar trend as that shown by the low-z quasars, i.e. an anticorrelation of EW(Fe II $\lambda\lambda$ 4434–4684)/EW(H β) versus EW([O III] λ 4959 + λ 5007)/EW(H β), with radio-loud quasars having on average smaller values of EW(Fe II $\lambda\lambda$ 4434–4684)/EW(H β) than radio-quiet quasars at any given value of EW([O III] λ 4959 + λ 5007)/EW(H β).

Recently Wang et al. (1996b) studied the relation between optical Fe II strength and properties of the UV spectra for 53 low-z ($z \leq 0.2$) quasars and found that there is a significant anticorrelation between the equivalent widths of optical Fe II $\lambda\lambda4434-4684$ and C IV $\lambda1549$. We examine whether the high-z quasars follow this anticorrelation (Table 3 and Figure 6). It is perhaps expected that the high-z quasars would have smaller $EW(C \text{ IV } \lambda 1549)$ than low-z guasars simply because of the known anticorrelation between $EW(C \text{ IV } \lambda 1549)$ and UV continuum luminosity (Baldwin effect: Baldwin 1977; Baldwin et al. 1978). Not as evident perhaps is that, except for 0933+733, the EW(Fe II $\lambda\lambda4434-4684$), appears to show the same range of values as do the low-z quasars at comparable low values of $EW(C \text{ IV }\lambda 1549)$. However, five of the remaining seven high-z quasars (B21225+317, 1246-057, S40636+68, B1422+231, and PKS 1937-101) have smaller EW (Fe II $\lambda\lambda4434-4684$) than any of the low-z quasars with comparable $EW(C \text{ IV } \lambda 1549)$ (see the lower-left region of the diagram in Figure 6), thus, adding the high-z sample to the low-z sample appears to decrease somewhat the significance of the anticorrelation between EW (Fe II $\lambda\lambda4434-4684$) versus EW (C IV $\lambda1549$), (although it is possible that not having a less luminous high-z sample may cause a selection effect). We thus consider it possible that the Fe II $\lambda\lambda$ 4434–4684 emitting region may not have a physical link directly with the C IV λ 1549 emitting region. However, it seems clear that there is no object with large EWs in both Fe II $\lambda\lambda4434-4684$ and C IV $\lambda1549$, and furthermore, the upper bound of EW (Fe II $\lambda\lambda4434-4684$) still decreases with increasing $EW(C \text{ IV } \lambda 1549)$ for the combined high-z and low-z samples. Hence, it is suggested that there may still be an indirect relation between the Fe II $\lambda\lambda$ 4434–4684 and C IV $\lambda 1549$ regions.

In summary, the relations among the emission-line properties shown in Figures 5 and 6 appear to be valid for both the low-z and high-z quasars with only a few exceptions. This implies that the emission mechanism and the physical properties of the emission-line region in high-z quasars may not be significantly different from those in low-z quasars.

⁴We note that a radio-loud high-z (z = 2.09) quasar 1331+170 also appears to lie within the locus of values found for the low-z radio-loud quasars (i.e., 1331+170 appears to have "quite weak" optical Fe II emission and $EW([O \text{ III}] \lambda 4959 + \lambda 5007)/EW(\text{H}\beta) \sim 0.7$ (Carswell *et al.* 1991).

We are very grateful to the staff of the UH 2.2 m telescope. In particular, we would like to thank Klaus Hodapp for his encouragement and Andrew Pickles for his technical support and assistance with the observations. This work was financially supported in part by Grants-in Aid for Scientific Research (Nos. 07044054 and 09640311) from the Japanese Ministry of Education, Science, Sports, and Culture and by the Foundation for Promotion of Astronomy, Japan. TM thanks the support of Research Fellowships from the Japan Society for the Promotion of Science for Young Scientists. All the figures in this paper were prepared with GP, the graph plotting tool developed by Keiichi Edamatsu. This research has made use of the NASA/IPAC Extragalactic Database (NED) and the NASA Astrophysics Data System Abstract Service.

REFERENCES

- Baldwin, J. A. 1977, ApJ, 214, 679
- Baldwin, J. A., Burke, W. L., Gaskell, C. M., & Wampler, E. J. 1978, Nature, 273, 431
- Bechtold, J., et al. 1994, AJ, 108, 374
- Boroson, T. A., & Oke, J. B. 1984, ApJ, 281, 535
- Boroson, T. A., & Green, R. F. 1992, ApJS, 80, 109
- Bregman, J. N. 1990, A&A Rev., 2, 125
- Carswell, R. F., et al. 1991, ApJ, 381, L5
- Collin-Souffrin, S., Hameury, J.-M., & Joly, M. 1988, A&A, 205, 19
- Elias, J. H., Frogel, J. A., Matthews, K., & Neugebauer, G. 1982, AJ, 87, 1029
- Elston, R., Thompson, K. L., & Hill, G. J. 1994, Nature, 367, 250 (ETH)
- Fang, Y., & Crotts, A. P. S. 1995, ApJ, 440, 69
- Francis, P. J., Hewett, P. C., Foltz, C. B., Chaffee, F. H., Weymann, R. J., & Morris, S. L. 1991, ApJ, 373, 465
- Gaskell, C. M. 1982, ApJ, 263, 79
- Hamann, F., & Ferland, G. 1993, ApJ, 418, 11
- Hammer, F., Rigaut, F., Angonin-Willaime, M.-C., & Vanderriest, C. 1995, A&A, 298, 737
- Hill, G. J., Thompson, K. L., & Elston, R. 1993, ApJ, 414, L1
- Hodapp, K.-W., Hora, J. L., Irwin, E., & Young, T. 1994, PASP, 106, 87
- Hora, J. L., & Hodapp, K.-W. 1996, Observers' Guide for KSPEC
- Jim, K. T. C., et al. 1997, PASP, in preparation
- Joly, M. 1991, A&A, 242, 49
- Junkkarinen, V. T., Burbidge, E. M., & Smith, H. E. 1987, ApJ, 317, 460

- Lançon, A., & Rocca-Volmerange, B. 1992, A&AS, 96, 593
- Lípari, S., Terlevich, R., & Macchetto, F. 1993, ApJ, 406, 451
- Kawara, K., Murayama, T., Taniguchi, Y., & Arimoto, N. 1996, ApJ, 470, L85
- Kinney, A. L., Rivolo, A. R., & Koratkar, A. P. 1990, ApJ, 357, 338
- Kwan, J., & Krolik, J. H. 1981, ApJ, 250, 478
- Malkan, M., & Sargent, W. L. W. 1982, ApJ, 254 22
- Maoz, D., et al. 1993, ApJ, 404, 576
- Mushotzky, R., & Ferland, G. J. 1984, ApJ, 278, 558
- Netzer, H., & Wills, B. J. 1983, ApJ, 275, 445
- Osterbrock, D. E. 1989, Astrophysics of Gaseous Nebulae and Active Galactic Nuclei (Mill Valley: University Science Books)
- Phillips, M. M. 1977, ApJ, 215, 746
- Phillips, M. M. 1978, ApJS, 38, 187
- Sanders, D. B., Phinney, E. S., Neugebauer, G., Soifer, B. T., & Matthews, K. 1989, ApJ, 347, 29
- Sargent, W. L. W., Boksenberg, A., & Steidel, C. C. 1988, ApJS, 68, 539
- Sargent, W. L. W., Steidel, C. C., & Boksenberg, A. 1989, ApJS, 69, 703
- Schultz, H. 1992, in Physics of Active Galactic Nuclei, ed. W. J. Duschl & S. J. Wagner (Berlin: Springer), 235
- Sergeev, S. G., Pronik, V. I., Malkov, Y. F., & Chuvaev, K. K. 1997, A&A, 320, 405
- Steidel, C. C., & Sargent, W. L. W. 1991, ApJ, 382, 433
- Steiner, J. E. 1981, ApJ, 250, 469
- Taniguchi, Y., Arimoto, N., Murayama, T., Evans, A. S., Sanders, D. B., & Kawara, K. 1996, to appear in the proceedings on Quasar Hosts held in Tenerife, Spain (September 24–27, 1996)
- Taniguchi, Y., Murayama, T., Kawara, K., & Arimoto, N. 1997, PASJ, 49, 419
- Turnshek, D. A., et al. 1994, ApJ, 428, 93
- Véron-Cetty, M.-P., & Véron, P. 1996, ESO Scientific Report, No. 17
- Wamsteker, W., et al. 1990, ApJ, 354, 446
- Wang, T., Brinkmann, W., & Bergeron, J. 1996a, A&A, 309, 81
- Wang, T., Zhou, Y., & Gao, A. 1996b, ApJ, 457, 111
- Wilkerson, M. S., Coleman, G., Gilbert, G., Strittmatter, P. A., Williams, R. E., Baldwin, J. A., Carswell, R. F., & Grandi, S. A. 1978, ApJ, 223, 364
- Wilkes, B. J. 1984, MNRAS, 207, 73

- Wills, B. J., Netzer, H., & Wills, D. 1985, ApJ, 288, 94
- Yoshii, Y., Tsujimoto, T., & Nomoto, K. 1996, ApJ, 462, 266
- Zheng, W., & O'Brien, P. T. 1990 ApJ, 353, 433
- Zheng, W., Fang, L. Z., & Binette, L. 1992, ApJ, 392, 74

This preprint was prepared with the AAS ${\rm IAT}_{\rm E}{\rm X}$ macros v4.0.

Fig. 1.— Comparison of the observed-frame *IHK* spectra of S40636+68 (solid line) and the LBQS composite spectrum of Francis *et al.* (1991; dashed line). The upper panel shows the atmospheric transmission for Mauna Kea produced using the program IRTRANS4. These data were obtained from the UKIRT worldwide web pages (http://www.jach.hawaii.edu/UKIRT/home.html).

Fig. 2.— The combined optical and near-infrared spectra of S40636+68 from the literature plus our *IHK*-band spectra. The best power-law fit to the optical–infrared continuum is indicated by the solid line. The dotted line is the LBQS composite spectrum (Francis *et al.* 1991).

Fig. 3.— The solid line shows our observed-frame K-band spectrum of S40636+68 and that of Elston *et al.* (1994) (dashed line). The spectrum of Elston *et al.* (1994) is scaled by a factor of two for comparison. The spike feature marked by 'X' is caused by residual atmospheric absorption. The center positions of H β , [O III] $\lambda\lambda$ 4959, 5007, and the Fe II multiplet 42 are indicated by marks. A redshift of z = 3.2 is assumed. The upper panel shows the atmospheric transmission.

Fig. 4.— The profile fitting of the K-band spectrum. The synthesized spectrum is over-plotted by the dashed line on the original spectrum (solid line). Note that the flux is multiplied by (1+z) for deredshifting. A linear continuum and each emission-line component are also shown.

Fig. 5.— Diagram between equivalent width ratios of $EW([O III] \lambda 5007 + \lambda 4959)/EW(H\beta)$ and $EW(Fe II \lambda \lambda 4434-4684)/EW(H\beta)$ for low-z (small symbols) and high-z quasars (large symbols). Sample data are compiled from Boroson & Green (1992), Hill *et al.* (1993), Elston *et al.* (1994), Kawara *et al.* (1996), Taniguchi *et al.* (1997). Radio-quiet quasars, flat-spectrum radio-loud quasars, and steep-spectrum radio-loud quasars are shown by open circles, filled circles, and filled squares, respectively. B21225+317 (radio-loud) is shown by the filled triangle because its radio spectrum is unknown.

Fig. 6.— Diagram between equivalent width of $EW(C \text{ IV }\lambda 1549)$ and $EW(\text{Fe II }\lambda\lambda 4434-4684)$. Large symbols are high-z quasars listed in Table 3 and small symbols are low-z quasars studied by Wang *et al.* (1996b). Radio-quiet quasars, flat-spectrum radio-loud quasars, and steep-spectrum radioloud quasars are shown by open circles, filled circles, and filled squares, respectively. B21225+317 (radio-loud) is shown by the filled triangle because its radio spectrum is unknown.

TABLE 1. Journal of observations for the published spectra of S4 0636+68.

Band	Reference	Observing Date	Telescope ^a	Aperture
Optical	Sargent <i>et al.</i> 1989	1987 Oct 19	Hale5	1'' slit
Optical	Bechtold <i>et al.</i> 1994	1989 Nov 2–3	SO2.3	$4''_{.5}$ slit
IJ	Bechtold <i>et al.</i> 1994	1989 Dec 12	MMT	3″
K	Elston <i>et al.</i> 1994	1992 Dec	KPNO2.1	Not reported
IJHK	This study	1996 Apr 7	UH2.2	0".96 slit

^aHale5 — Hale 5 m Telescope + Double Spectrograph;

SO2.3 — Steward Observatory 2.3 m Telescope + Boller & Chivens Spectrograph;

MMT — Multiple Mirror Telescope + Germanium Spectrometer;

KPNO2.1 — Kitt Peak National Observatory 2.1 m Telescope + Cryogenic Spectrometer;

UH2.2 — University of Hawaii 2.2 m Telescope + KSPEC.

Line	$F/F({ m H}eta)^{ m a,b}$	$\frac{EW(\text{rest})^{\text{c}}}{(\text{Å})}$	$FWHM^{\rm d}$ (km s ⁻¹)	$\frac{FWHM_{\rm cor}^{\rm e}}{\rm (km \ s^{-1})}$					
Local linear continuum									
$\mathrm{H}\beta^{\mathrm{a}}$	1	32 ± 4	4996	4971					
$[O III] \lambda 5007$	0.16 ± 0.07	5.5 ± 2	2275	2225					
Fe II $\lambda\lambda 3500-6000^{f}$ 3.5 ± 1.1		115 ± 32		• • •					
Fe II $\lambda\lambda 4434-4684^{\text{g}}$ 0.83 ± 0.26		26 ± 7							
[O II] $\lambda 3727$ < 0.30 ^h		$< 7.0^{h}$		(1000)					
	Global p	ower-law continuum							
$\mathrm{H}\beta^\mathrm{b}$	1	42 ± 6	5920	5900					
$[O III] \lambda 5007$	0.19 ± 0.09	8.5 ± 4	3592	3561					
Fe II $\lambda\lambda 3500-6000^{\rm f}$	4.7 ± 1.1	189 ± 34		• • •					
Fe II $\lambda\lambda4434$ –4684 ^g	1.1 ± 0.25	43 ± 8							
$[O II] \lambda 3727$	$< 0.24^{\rm h}$	$< 7.1^{\rm h}$		(1000)					

TABLE 2. Emission-line properties of S4 0636+68.

 ${}^{\mathrm{a}}F(\mathrm{H}\beta) = (2.3 \pm 0.3) \times 10^{-14} \text{ erg s}^{-1} \text{ cm}^{-2}.$ ${}^{\mathrm{b}}F(\mathrm{H}\beta) = (2.9 \pm 0.4) \times 10^{-14} \text{ erg s}^{-1} \text{ cm}^{-2}.$

^cRest frame equivalent width.

^dFull width at half maximum.

^eFull width at half maximum corrected for instrumental broadening.

^fTo compare with the sample of Wills *et al.* (1985).

^gTo compare with the sample of Hill *et al.* (1993).

^h3- σ upper limits assuming $FWHM_{cor} = 1000$ km s⁻¹.

Name	Redshift	$M_B{}^{\mathrm{a}}$	$\frac{EW(C \text{ IV } \lambda 1549)}{(\text{\AA})}$	$\begin{array}{c} EW ({\rm Fe~II})^{\rm b} \\ ({\rm \AA}) \end{array}$	References
B2 1225+317 1246-057 0933+733 S4 0636+68 S5 0014+81 B 1422+231 PKS 1937-101	$2.219 \\ 2.244 \\ 2.551 \\ 3.200 \\ 3.398 \\ 3.620 \\ 3.787$	$\begin{array}{r} -30.0 \\ -29.1 \\ -29.5 \\ -31.3 \\ -31.7 \\ -30.7 \\ -30.3 \end{array}$	6.9 29 29 14 12 61 ^e 26 ^e	$\begin{array}{c} 42^{\rm c} \\ 58^{\rm c} \\ 185^{\rm c} \\ 26 \\ 90^{\rm d} \\ 6.6^{\rm f} \\ < 29 \end{array}$	$1, 2 \\ 2, 3 \\ 2, 4 \\ 5, 6 \\ 5, 7, 8 \\ 9, 10 \\ 11, 12$

TABLE 3. Rest frame equivalent width of C IV λ 1549 and Fe II for high-z quasars.

^aThe absolute B magnitude from Véron-Cetty & Véron (1996).

^bEquivalent width of optical Fe II measured between 4434 Å and 4684 Å.

^cThese values were derived from the flux ratios of Fe II/H β tabulated in Hill *et al.* (1993) and the linear continuum shown in their Figure 2.

^dRough estimate by us from the spectrum given in Elston *et al.* (1994).

^eThese values were measured by us from the spectra in the literature.

^fThis value is re-measured by us because Kawara *et al.* (1996) did not provide the equivalent width of Fe II.

References for Table 3.

Wilkerson et al. 1978; (2) Hill et al. 1993; (3) Junkkarinen et al. 1987; (4) Steidel & Sargent 1991;
 (5) Sargent et al. 1989; (6) This study; (7) Sargent et al. 1988; (8) Elston et al. 1994; (9) Hammer et al. 1995; (10) Kawara et al. 1996; (11) Fang & Crotts 1995; (12) Taniguchi et al. 1997.